RESEARCH ARTICLE OPEN ACCESS

Development and Screening of One-Part Geopolymer suitable for Extrusion-Based 3D Printing Applications: Effects of Water-to-Binder Ratio and Sucrose Retarder Content

Prasad Barve*, Deep Upadhyaya**, Santosh Shah***
**Research Scholar, Department of Civil Engineering, Gujarat Technological University, Ahmedabad 382424, Gujarat, India*
*** Assistant Professor, Department of Civil Engineering, Government Engineering College, Godhra 389001, Gujarat, India*
**** Director of Construction, OM Group, Illinois 60527, United States of America;*
Corresponding author: (Deep Upadhyaya)

ABSTRACT
This study develops and optimizes a one-part geopolymer concrete for extrusion-based three-dimensional (3D) printing using fly ash (FA), ground granulated blast-furnace slag (GGBS), sodium metasilicate anhydrous powder as the sole solid activator, fine sand with a maximum particle size of 600 µm, and sucrose as a setting retarder. Twenty-seven mixtures were produced by varying the FA:GGBS ratio (90:10, 70:30 and 50:50), water-to-binder ratio (0.30, 0.35 and 0.40), and sucrose dosage (0.5%, 1.0% and 1.5% by precursor mass), while the activator content and aggregate-to-binder ratio were fixed at 10% and 1.5, respectively. Mini-slump/flow, 10-min flow-retention, setting time, density and compressive strength were used to screen the mixtures. The 50:50 FA: GGBS mixture with w/b = 0.35 and 1.0% sucrose (BM-15) provided the most balanced response, with 156 mm flow before drop, 141 mm after drop, 15 mm loss after 10 min, 151 min initial setting, 196 min final setting, 2180 kg/m³ density, and 24.58 and 36.42 MPa compressive strengths at 7 and 28 days, respectively. The results demonstrate that printable geopolymer design requires simultaneous control of flowability and structural build-up rather than maximization of either parameter alone. Literature-based analysis further shows how precursor chemistry, aggregate-to-binder ratio, activator dosage, water content and retarder dosage govern pumpability, extrudability, buildability, shape retention and open time. BM-15 is therefore identified as the optimum formulation within the investigated design space for subsequent extrusion-based concrete 3D-printing validation.

***Keywords* –** concrete 3D printing, compressive strength, flowability and setting time, one-part geopolymer, printability

---

Date of Submission: 01-09-2026 Date of acceptance: 11-09-2026

I. INTRODUCTION

Additive manufacturing is changing the construction process from a formwork-dependent operation to a digitally controlled, layer-wise deposition process. In extrusion-based concrete 3D printing, a fresh cementitious or alkali-activated material must pass through a sequence of coupled operations comprising mixing, pumping, extrusion and deposition. The material is therefore required to satisfy apparently contradictory conditions: sufficiently low resistance to flow during pumping and extrusion, followed by sufficiently rapid structural build-up after deposition to support subsequent layers. Recent reviews consistently identify pumpability, extrudability and buildability as the principal material-level requirements, with shape retention and open time acting as time-dependent constraints on the printable window [1-5].

Geopolymer and alkali-activated binders are attractive for 3D printing because industrial by-products such as fly ash and GGBS can replace Portland clinker while providing a chemically reactive binder system. The combination of fly ash and slag is especially relevant because the two precursors contribute complementary characteristics. Spherical fly ash particles can promote flowability and packing, whereas the calcium-rich and generally more reactive GGBS fraction can accelerate reaction and structural build-up. Consequently, changing the FA:GGBS ratio influences both the fresh-state rheology and the development of hardened strength [6-11].

One-part geopolymer systems are particularly attractive for construction because the reactive ingredients are supplied in a dry premixed form and water is added at the point of use. This simplifies handling relative to conventional two-part geopolymer systems that require separate storage and metering of alkaline solutions. Studies on just-add-water geopolymer concretes have shown that solid sodium silicate or related solid activators can produce mixtures with useful printability and mechanical performance, although rapid reaction and loss of open time remain important limitations [7, 8]. The use of a solid activator is therefore highly compatible with a practical dry-feed manufacturing route, provided that the activator dissolves adequately during mixing and the subsequent geopolymerization rate is controlled.

The present investigation addresses this formulation problem through a systematic 27-mixture screening program. The precursor ratio, water-to-binder ratio and sucrose retarder dosage were varied while the sodium metasilicate anhydrous activator content and sand-to-binder ratio were held constant. The experimental purpose was not simply to obtain maximum slump flow or maximum strength, but to identify a balanced mixture that maintains adequate flow, acceptable flow retention, a suitable setting-time window and adequate hardened strength for 3D printing.

The work is significant because conventional concrete mix-design criteria cannot be transferred directly to extrusion-based 3D printing. A highly fluid material may pump readily but deform after deposition, whereas a highly stiff material may retain its shape but generate excessive extrusion pressure or discontinuous filaments. Recent literature has emphasized the need for a printable window in which rheology evolves from a pumpable state to a buildable state over the duration of printing [1, 4, 5]. Simple field-oriented tests such as slump and slump flow have also been shown to provide useful first-stage screening information for one-part geopolymer mixtures [12].

Accordingly, the objectives of this study are to: (i) develop a one-part FA–GGBS geopolymer concrete activated with sodium metasilicate anhydrous powder; (ii) quantify the effects of precursor ratio, water-to-binder ratio and sucrose dosage on slump/flow and flow retention; (iii) evaluate the corresponding setting-time window; (iv) compare density and compressive strength; and (v) interpret the combined fresh and hardened responses in terms of pumpability, extrudability, buildability, shape retention and open time.

II. LITERATURE REVIEW AND THEORETICAL BASIS

1.1 Printability as a coupled material-process requirement

Extrusion-based 3D concrete printing differs from casting because the material is required to perform without a mold. The fresh material must therefore be capable of being transported through a hose, forced through a nozzle, deposited continuously, and stacked into a self-supporting geometry. Pumpability is primarily associated with resistance to flow in the delivery system, while extrudability concerns the continuity and geometric quality of the filament as it leaves the nozzle. Buildability concerns the ability of deposited layers to resist deformation under their own weight and the weight of subsequent layers [1, 3-5].

The rheological parameters most often used to describe this behaviour are static yield stress, dynamic yield stress, plastic viscosity and thixotropy. During pumping and extrusion, relatively low dynamic yield stress and plastic viscosity are beneficial because they reduce the pressure required to move the mixture. Immediately after deposition, however, a sufficiently high structural yield stress and rapid structural rebuilding are required to prevent lateral spreading and collapse. This transition is central to printable-material design [1, 4, 5, 13].

Open time is another critical variable. A mixture can possess excellent instantaneous flowability but still be unsuitable for printing if its rheological properties change rapidly after mixing. In geopolymer systems, alkali activation and dissolution–polycondensation reactions can cause a strong time-dependent increase in stiffness. Retarders, changes in activator chemistry, lower solution alkalinity, temperature control and print-head activation are therefore among the strategies reported to extend the usable printing window [7, 8, 14-17].

2.2 One-part geopolymer concrete for 3D printing

One-part geopolymer concrete uses a dry solid activator that is blended with the precursor and aggregate before water is added. This approach is analogous to a conventional dry-mix product and offers logistical advantages compared with liquid-activator systems. Bong et al. demonstrated ambient-temperature curing of a just-add-water geopolymer based on fly ash and slag with solid sodium silicate powders, showing that the solid-activator route can provide promising open time, buildability and mechanical performance [7]. Muthukrishnan et al. subsequently examined the rheo-chemical development of one-part geopolymer concrete and demonstrated that activator content, thixotropic additives and sucrose can influence the time-dependent rheology and buildability [8].

The present material system follows a similar broad one-part concept but uses sodium metasilicate anhydrous powder as the sole activator, with an activator content of 10% by binder mass. This fixed dosage allows the experimental program to focus on the interaction between precursor chemistry, water and retarder. It should be emphasized that activator dosage was not experimentally varied in the present study; therefore, conclusions about activator content are literature-supported implications rather than direct experimental comparisons.

2.3 Role of fly ash and GGBS

Fly ash and GGBS contribute differently to geopolymerization. The generally spherical morphology of fly ash can reduce interparticle friction and improve flowability, whereas GGBS contains reactive calcium-bearing phases that can promote faster structural development and higher early strength. Reviews of geopolymer 3D printing repeatedly report that increasing the proportion of slag tends to increase stiffness and structural build-up, while higher fly ash contents generally favour workability [2, 9, 10].

The effect is not purely physical. Calcium supplied by GGBS can alter the reaction-product assemblage and promote calcium-containing aluminosilicate hydrate phases alongside sodium aluminosilicate hydrate products. The resulting hybrid gel structure can increase early rigidity and improve layer retention. For 3D printing, this chemical contribution is important because buildability depends not only on the initial yield stress but also on the rate at which the material develops load-bearing capacity after deposition [8, 9, 15].

2.4 Water-to-binder ratio

Water controls both workability and the degree of dilution of the reactive system. Increasing w/b generally increases flow and reduces the resistance to pumping and extrusion. However, excessive water can delay structural recovery, increase slump/flow, promote deformation and reduce hardened density and strength. In one-part geopolymer concrete, Tran et al. reported a printable region based on combined slump and slump-flow measurements and identified water/binder ratio as a major parameter controlling the printable window [12].

2.5 Retarder dosage and open time

Sucrose is frequently used as a retarding agent in geopolymer formulations because it can interact with dissolved species and interfere with early reaction processes, thereby delaying structural stiffening. The effect, however, is dosage-dependent: excessive retardation can increase the open time beyond the practical requirement for rapid layer stacking, whereas insufficient retardation may cause premature stiffness and loss of extrudability.

2.6 Aggregate-to-binder ratio and particle size

Aggregate characteristics strongly affect pumpability, extrusion pressure, filament continuity and surface quality. Larger or poorly graded particles can increase blockage risk, while excessively fine aggregate increases surface area and water demand. Recent reviews identify aggregate size, shape, grading and aggregate-to-binder ratio as major controls on pumpability and rheology [3-5]. The present study uses fine sand with a maximum particle size of 600 µm and a fixed aggregate-to-binder ratio of 1.5.

The literature nevertheless indicates that increasing aggregate-to-binder ratio can reduce paste demand and potentially improve dimensional stability, but excessive aggregate loading may increase friction and extrusion pressure. A 2026 study on one-part geopolymer concrete reported that a higher aggregate-to-binder ratio of 1.9 could provide a favorable balance between extrudability and buildability while reducing binder consumption [18]. This supports the importance of aggregate optimization but does not imply that 1.9 is superior to the present 1.5 ratio for the present materials, nozzle and processing conditions.

III. MATERIALS AND METHODS

3.1 Materials

The geopolymer concrete was formulated using fly ash and GGBS as the aluminosilicate precursors. The precursor ratio was varied at 90:10, 70:30 and 50:50 FA:GGBS by mass. Sodium metasilicate anhydrous powder was used as the sole solid alkaline activator at 10% of binder mass. Fine sand with a maximum particle size of 600 µm was used as aggregate. The aggregate-to-binder ratio was fixed at 1.5:1. Water-to-binder ratios of 0.30, 0.35 and 0.40 were investigated. Sucrose powder was used as a retarder at 0.5%, 1.0% and 1.5% of precursor mass. These proportions generated 27 mixtures.

The formulation philosophy was intentionally centered on a one-part dry mixture. The solid precursor, activator, aggregate and sucrose can therefore be premixed and supplied as a dry product, with water added immediately before printing. This configuration is attractive for field implementation because it avoids handling and metering a concentrated liquid alkaline solution. Similar just-add-water approaches have been investigated in previous 3D-printable geopolymer research [7, 8].

3.2 Experimental matrix

Experimental mix proportions for the 27 mixtures are shown in Table 1. For each mix, the binder mass was 400 g. Consequently, the water masses were 120, 140 and 160 g for w/b ratios of 0.30, 0.35 and 0.40, respectively; sand mass was 600 g and activator mass was 40 g. The precursor masses were 360/40 g, 280/120 g and 200/200 g for the 90:10, 70:30 and 50:50 FA:GGBS ratios, respectively.

Table 1. Experimental mix proportions for the 27 mixtures.

Mix	**FA:GGBS**	**w/b**	**Sucrose (%)**	**Sand (g)**	**Water (g)**	**Activator (g)**	**A/B**
BM-1	90:10	0.30	0.5	600	120	40	1.5
BM-2	70:30	0.30	0.5	600	120	40	1.5
BM-3	50:50	0.30	0.5	600	120	40	1.5
BM-4	90:10	0.35	0.5	600	140	40	1.5
BM-5	70:30	0.35	0.5	600	140	40	1.5
BM-6	50:50	0.35	0.5	600	140	40	1.5
BM-7	90:10	0.40	0.5	600	160	40	1.5
BM-8	70:30	0.40	0.5	600	160	40	1.5
BM-9	50:50	0.40	0.5	600	160	40	1.5
BM-10	90:10	0.30	1.0	600	120	40	1.5
BM-11	70:30	0.30	1.0	600	120	40	1.5
BM-12	50:50	0.30	1.0	600	120	40	1.5
BM-13	90:10	0.35	1.0	600	140	40	1.5
BM-14	70:30	0.35	1.0	600	140	40	1.5
BM-15	50:50	0.35	1.0	600	140	40	1.5
BM-16	90:10	0.40	1.0	600	160	40	1.5
BM-17	70:30	0.40	1.0	600	160	40	1.5
BM-18	50:50	0.40	1.0	600	160	40	1.5
BM-19	90:10	0.30	1.5	600	120	40	1.5
BM-20	70:30	0.30	1.5	600	120	40	1.5
BM-21	50:50	0.30	1.5	600	120	40	1.5
BM-22	90:10	0.35	1.5	600	140	40	1.5
BM-23	70:30	0.35	1.5	600	140	40	1.5
BM-24	50:50	0.35	1.5	600	140	40	1.5
BM-25	90:10	0.40	1.5	600	160	40	1.5
BM-26	70:30	0.40	1.5	600	160	40	1.5
BM-27	50:50	0.40	1.5	600	160	40	1.5

3.3 Slump and slump flow testing

Slump and slump-flow measurements were performed in accordance with IS 4031 (Part 7):1988 using a flow-table apparatus conforming to IS 5512:1983 and a mini-slump cone 50 mm high with top and bottom diameters of 70 and 100 mm, respectively. The initial flow was recorded before dropping the flow table, the post-drop flow was recorded after the specified table action, and the flow was measured again after 10 min to quantify time-dependent retention. The percentage reduction was calculated as the reduction in flow divided by the post-drop flow, expressed as a percentage. These measurements were used as practical indicators of initial workability, flow retention and the time window available for printing.

3.4 Setting time

Initial and final setting times were recorded for all 27 mixtures pastes' (without sand) using a Vicat apparatus as per IS 4031 (Part-5):1988. The setting-time window was calculated as the difference between final and initial setting times.

3.5 Density and compressive strength

Mold-cast cube specimens of 50 × 50 × 50 mm³ were cured at laboratory ambient conditions of 27 ± 2 °C and 65 ± 5% relative humidity. Compressive strength was measured at 7 and 28 days using a compression testing machine with a maximum load capacity of 3000 kN. The loading rate was 0.583 kN/s in accordance with IS 516 (Part 1/Sec 1):2021. Density was determined at 28 days.

IV. RESULTS AND DISCUSSION

4.1 Overall workability response

The 27-mix screening demonstrates a pronounced dependence of post-drop flow on water content. At w/b = 0.30, post-drop flow ranged from 132 to 141 mm at 0.5% sucrose, 129 to 139 mm at 1.0% sucrose and 126 to 136 mm at 1.5% sucrose. The qualitative assessment classifies all w/b = 0.30 mixtures as too low flow except BM-3, which was considered marginal. This establishes that the lowest water level did not provide sufficient flow for a robust printing process.

At w/b = 0.35, the post-drop flow ranged from 143 to 162 mm. This intermediate water level eliminated the very low-flow condition while avoiding the largest spreads observed at w/b = 0.40. BM-15, with a 50:50 FA:GGBS ratio and 1.0% sucrose, had a post-drop flow of 141 mm and a 10-min flow of 126 mm; the supplied table records 141 mm as the slump/flow after drop and 15 mm reduction after 10 min, corresponding to 9.62% reduction.

At w/b = 0.40, the post-drop flow increased substantially, reaching 174 mm for BM-7 and 177 mm for BM-16. Such high initial flow is not necessarily advantageous for extrusion printing. The material may be easier to pump, but the deposited filament can spread laterally before sufficient structural rebuilding occurs. The supplied assessments consequently classify these mixtures mainly as low retention, with BM-7 showing excessive reduction. This behaviour is consistent with the fundamental pumpability–buildability trade-off described in the literature [1, 3-5]. Effect of water-to-binder ratio, FA:GGBS precursor ratio and sucrose dosage on slump/flow after drop is shown in Fig. 1.

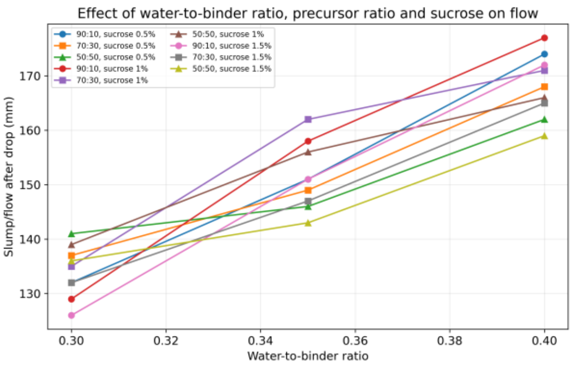

Figure 1. Effect of water-to-binder ratio, FA:GGBS precursor ratio and sucrose dosage on slump/flow after drop.

4.2 Effect of precursor ratio

The precursor ratio modifies both the physical packing and the chemical reaction rate. At w/b = 0.35 and 0.5% sucrose, the post-drop flow decreased from 151 mm at 90:10 FA:GGBS (BM-4) to 149 mm at 70:30 (BM-5) and 146 mm at 50:50 (BM-6). A similar trend is observed at 1.0% sucrose, where BM-13, BM-14 and BM-15 exhibited 158, 162 and 156 mm, respectively. At 1.5% sucrose, the corresponding values were 151, 147 and 143 mm. Thus, the influence of precursor ratio is real but is coupled with water and retarder dosage.

Increasing GGBS generally increases the amount of reactive calcium-bearing material and can promote faster structural development. In a printing context, this can be beneficial because the freshly deposited filament needs to acquire load-bearing capacity rapidly. However, excessive structural build-up can shorten open time and increase the risk of hose or nozzle blockage. Published studies on one-part and alkali-activated 3D-printable systems similarly report that the FA/GGBS balance governs yield stress, setting behaviour and buildability [7-10, 15].

The present results indicate that the 50:50 FA:GGBS ratio is particularly effective when combined with w/b = 0.35 and 1.0% sucrose. Importantly, the optimum is not produced by precursor ratio alone. BM-3 and BM-12, which also contain 50:50 FA:GGBS, are classified as marginal or too low flow at w/b = 0.30. BM-24 at 50:50 and 1.5% sucrose is classified as low retention. Therefore, the optimum is a multi-variable balance rather than a single-factor optimum.

4.3 Effect of water-to-binder ratio

Water-to-binder ratio produced the clearest systematic shift in initial flow. Increasing w/b from 0.30 to 0.35 increased the post-drop flow for all precursor and sucrose combinations. A further increase to 0.40 produced still higher post-drop flow. This confirms that water is the dominant short-term workability control in the investigated range.

From a pumping perspective, the higher flow at w/b = 0.40 would normally be favorable because less pressure is required to initiate and maintain movement. However, the 3D-printing process imposes an additional requirement: after leaving the nozzle, the filament must retain its geometry. The lower retention classifications at w/b = 0.40 indicate that the mixtures may be too fluid to develop sufficient shape stability during deposition. Literature on 3D printing consistently emphasizes that high fluidity alone cannot define printability [1,2,4,5].

At w/b = 0.30, the opposite problem occurs. The low flow values indicate insufficient mobility, which would increase extrusion pressure and potentially promote intermittent extrusion, surface tearing or nozzle blockage. Therefore, the intermediate w/b of 0.35 is the optimum. This is consistent with the findings of Tran et al., who reported that one-part geopolymer mixtures require an adequate water/binder ratio to enter a printable region defined jointly by slump and flow [11]. Average flow retained after 10 min at each water-to-binder ratio for the three sucrose dosages is shown in Fig. 2.

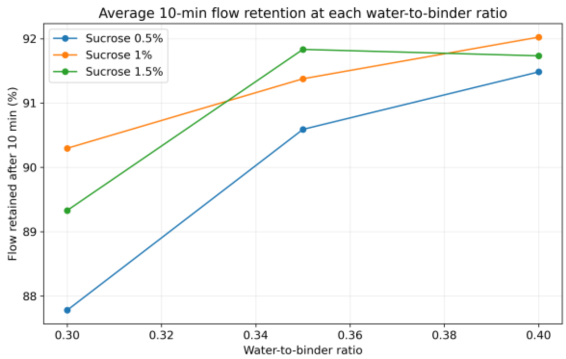

Figure 2. Average flow retained after 10 min at each water-to-binder ratio for the three sucrose dosages.

4.4 Effect of sucrose dosage

Increasing sucrose from 0.5% to 1.5% generally decreases the post-drop flow at a fixed water-to-binder ratio and precursor ratio, while extending the setting times. This indicates that sucrose successfully modifies the time-dependent reaction behavior. At w/b = 0.35 and 50:50 FA:GGBS, the post-drop flow decreased from 146 mm at 0.5% sucrose (BM-6) to 141 mm at 1.0% (BM-15) and 131 mm at 1.5% (BM-24). The corresponding flow reductions after 10 min were 13, 15 and 12 mm, respectively.

The most useful retarder dosage is therefore not the highest dosage. A retarder should provide enough open time for mixing, pumping and deposition while allowing structural build-up soon enough to support subsequent layers. Excessive retardation can leave lower layers insufficiently stiff during a fast-printing sequence. Conversely, too little retardation can cause premature stiffening before the material reaches the nozzle. The literature identifies this balance as one of the defining challenges of geopolymer 3D printing [7, 8, 14-17].

4.5 Ten-minute flow retention and open-time implications

The 10-min flow-retention results provide a practical indication of how quickly the fresh mixtures change after mixing. Across all mixtures, percentage reductions range from 7.83% to 13.14%. The lowest reduction was recorded for BM-18 (7.83%), whereas BM-2 showed the highest reduction (13.14%). BM-15 had a 9.62% reduction, which is neither the lowest nor the highest value. This is important because minimum flow loss is not the sole objective. A printable material needs controlled change: sufficient stability to resist spreading, but sufficient retained workability to complete extrusion.

The post-drop flow and 10-min flow should therefore be interpreted together. A mixture with a very low initial flow and small percentage reduction may remain unprintable because its initial resistance is too high. Similarly, a mixture with a very high initial flow and small reduction may remain too fluid for buildability. BM-15 occupies a middle position in both respects, supporting the conclusion that its suitability results from balance rather than from an extreme value of any single parameter.

4.6 Setting-time behavior

The setting-time results shown in Fig. 3 reveal the effect of both precursor chemistry and sucrose dosage. Initial setting times range from 112 min for BM-1 to 174 min for BM-27, while final setting times range from 157 to 222 min. The setting-time window remains comparatively narrow, between 43 and 48 min, indicating that the main change across the experimental matrix is the absolute time at which structural stiffening begins rather than a dramatic change in the duration between initial and final setting.

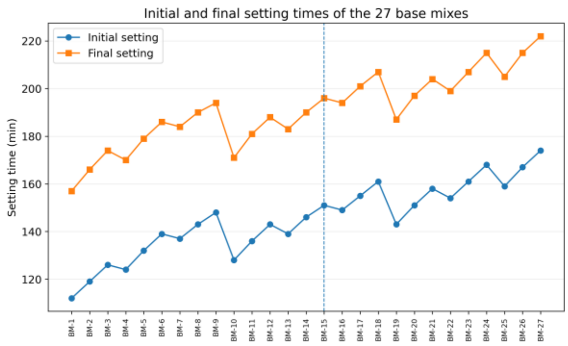

Figure 3. Initial and final setting times of the 27 mixtures

The low-sucrose series generally sets earlier than the higher-sucrose series. At 50:50 FA:GGBS, for example, initial setting increases from 126 min for BM-3 to 143 min for BM-12 and 158 min for BM-21 as sucrose increases from 0.5% to 1.5% at w/b = 0.30. At w/b = 0.35, the corresponding values are 139, 151 and 168 min for BM-6, BM-15 and BM-24. This demonstrates the combined effect of retarder dosage and precursor chemistry.

BM-15 has an initial setting time of 151 min, final setting time of 196 min and a 45-min setting-time window. The supplied assessment identifies it as optimum. From a printing perspective, this window is long enough to permit practical material preparation, transport and deposition while the absolute setting time is not so delayed that the lower layers would remain weak for an extended period. This interpretation is consistent with the broader literature showing that printable geopolymer systems require a controlled open time followed by sufficiently rapid structural development [7, 8, 12, 14].

4.7 Density and compressive strength

The seven- and 28-day compressive strengths of the 27 mixtures are shown in Fig. 4 and the relationship between 28-day density and compressive strength are shown in Fig. 5. The 28-day density values range from 2105 to 2180 kg/m³. BM-15 has the highest reported density of 2180 kg/m³. The relatively high density is consistent with the combined presence of fine sand, a relatively high aggregate-to-binder ratio of 1.5 and a reactive FA–GGBS binder system. The density results should be viewed as indicators of packing and hardened matrix compactness rather than direct measures of printability.

Seven-day compressive strengths range from 18.76 to 24.58 MPa, while 28-day strengths range from 29.94 to 36.42 MPa. BM-15 gives the highest value at both ages, with 24.58 MPa at 7 days and 36.42 MPa at 28 days. The 28-day strength increase relative to the 7-day value is 11.84 MPa, corresponding to approximately 48.2% growth relative to the 7-day value. This indicates continuing geopolymerization and matrix development under ambient curing.

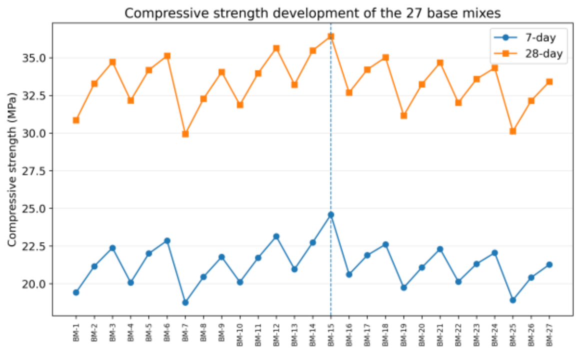

Figure 4. Seven- and 28-day compressive strengths of the 27 mixtures

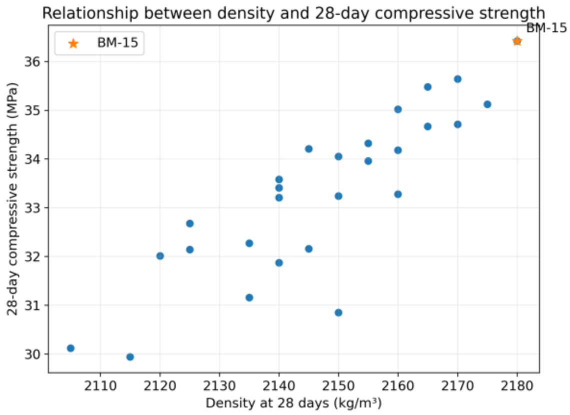

Figure 5. Relationship between 28-day density and compressive strength

The strength response is strongly influenced by the precursor ratio and water content. At w/b = 0.35 and 1.0% sucrose, the 28-day strength increases from 33.21 MPa for BM-13 (90:10 FA:GGBS) to 35.48 MPa for BM-14 (70:30) and 36.42 MPa for BM-15 (50:50). This trend is consistent with the role of GGBS in increasing calcium availability and accelerating the development of calcium-containing reaction products. The result also agrees with broader 3D-printable geopolymer literature in which slag addition is associated with higher early-age stiffness and strength [7, 9, 15, 18].

Increasing water to w/b = 0.40 generally reduces density and strength. At 1.0% sucrose, BM-15 at w/b = 0.35 reaches 36.42 MPa, whereas BM-18 at w/b = 0.40 reaches 35.02 MPa. The reduction is consistent with greater dilution and potentially greater capillary porosity after water consumption and drying. At w/b = 0.30, the strength can also be relatively high, but the flowability is inadequate for printing. This is another example of why hardened strength alone cannot be used to select a printable mix.

4.8 Integrated selection of BM-15

The optimum mixture must satisfy multiple constraints simultaneously. BM-15 uses 50:50 FA:GGBS, w/b = 0.35 and 1.0% sucrose. It provides 156 mm flow before drop, 141 mm flow after drop, 15 mm flow reduction after 10 min, and 9.62% reduction. Its initial and final setting times are 151 and 196 min, giving a 45-min setting-time window. Its density is 2180 kg/m³, with 7- and 28-day compressive strengths of 24.58 and 36.42 MPa, respectively.

The importance of BM-15 becomes clearer when neighboring formulations are considered. BM-12 has a higher 28-day strength of 35.64 MPa than many lower-performing mixtures but is classified as having poor flow at w/b = 0.30. BM-14 has a high strength of 35.48 MPa and acceptable setting behavior, but the manuscript identifies BM-15 as the optimum because its combined response is superior. BM-16 has higher initial flow at 177 mm but lower density and strength and a low-retention classification. BM-24 has a 47-min setting window but is judged low retention and has a lower 28-day strength of 34.32 MPa. Thus, BM-15 is not selected simply because it has the highest strength; it is selected because it lies in a balanced region of workability, retention, setting and strength.

This selection strategy is consistent with recent printable-geopolymer research. The literature increasingly treats printability as a process window rather than a single test value, requiring simultaneous consideration of flow, structural build-up, open time and hardened performance [1, 4, 5, 17]. The present study provides a practical screening route in which simple flow and setting tests identify a candidate mixture before full-scale printing trials.

4.9 Implications for pumpability

Pumpability refers to the ability of the material to travel through the delivery hose under a controllable pressure without segregation, excessive friction or blockage. Low dynamic yield stress and moderate plastic viscosity generally favor pumping [1, 3, 4]. For the present mixes, w/b = 0.30 is likely to require the greatest pumping pressure because the post-drop flow is low. The w/b = 0.40 mixes should be easier to pump, but their high flow raises concerns about downstream shape retention. BM-15 at w/b = 0.35 therefore represents a practical compromise between pressure demand and excessive fluidity.

The fine aggregate size of 600 µm also supports pumpability because it reduces the likelihood of particle bridging at a conventional small printing nozzle. Nevertheless, actual pump pressure cannot be quantified from slump-flow measurements alone. Pumpability should be confirmed experimentally using the selected pump, hose length, internal diameter, nozzle geometry and printing speed. Recent studies emphasize that material rheology and equipment configuration are coupled during pumping [3-5].

4.10 Implications for extrudability

Extrudability requires continuous discharge of the mixture with minimal tearing, discontinuity or segregation. A material that is too stiff may produce an irregular filament, while a highly fluid material may exit continuously but spread excessively after deposition. The post-drop flow values therefore provide a first-stage indication of whether the mixture is within a reasonable extrusion range, but visual filament inspection remains necessary.

BM-15's intermediate flow is favourable from this perspective. The mixture should be capable of flowing through the nozzle while retaining sufficient cohesion because the FA–GGBS combination provides a reactive binder skeleton and sucrose moderates early stiffening. The 600 µm maximum sand size further reduces the risk of nozzle obstruction. Similar material-level considerations are highlighted in recent reviews and experimental studies of geopolymer extrusion [1, 2, 5, 7, 15].

4.11 Implications for buildability and shape retention

Buildability is the ability of deposited material to retain its shape and support the load of subsequently deposited layers. It depends on static yield stress, structural build-up, elastic modulus, thixotropy and the time interval between layers. A mix can have good initial flow yet poor buildability if the structural rebuild rate is insufficient. Conversely, an extremely fast structural build-up can prevent continuous extrusion and cause cold joints or blockage [1, 8, 14-17].

The present BM-15 formulation is expected to have better buildability than the high-water mixtures because its w/b ratio is intermediate and its 50:50 FA:GGBS ratio provides a higher proportion of reactive slag than the 90:10 and 70:30 formulations. The 1.0% sucrose dosage also prevents excessively rapid stiffening. This balance is the principal basis for the manuscript's conclusion that BM-15 is the optimum candidate for printing.

However, because the results do not include a quantitative layer-stack test, the present manuscript should distinguish between demonstrated material suitability and direct printed buildability. The results demonstrate a favourable fresh-state window and hardened strength in cast specimens. Actual buildability should be validated by printing a multi-layer wall or cylindrical element and measuring layer deformation, dimensional deviation and maximum stable layer count. This distinction strengthens rather than weakens the scientific interpretation.

4.12 Implications for open time

Open time is the period over which the material remains sufficiently workable for pumping and extrusion. The setting-time and 10-min flow-retention results provide complementary information about this period. BM-15 maintains approximately 90.38% of its post-drop flow after 10 min and has an initial setting time of 151 min. The combination suggests a useful interval between initial mixing and the onset of final structural stiffening.

Recent studies have demonstrated alternative approaches for extending open time, including modified activator systems, nano-silica combinations, nanocellulose, temperature control and in-line activation [14-17, 19-21]. The present formulation deliberately uses a simple sucrose-retarded one-part system. This simplicity is an advantage for practical dry-mix manufacturing, provided that the actual printing window is confirmed under the intended equipment and ambient conditions.

4.13 Aggregate-to-binder ratio: literature-based interpretation

The aggregate-to-binder ratio was fixed at 1.5:1 and therefore does not constitute an independent variable in this study. A higher aggregate fraction generally lowers the volume of reactive paste available to lubricate the particles. This can reduce binder demand and improve dimensional stability, but it may also increase friction and extrusion pressure if the aggregate skeleton becomes too dominant. The optimum is therefore dependent on aggregate grading, nozzle size, particle morphology and binder rheology [3-5, 18].

Recent work by Ajayi et al. demonstrated the feasibility of a 1.9 aggregate-to-binder ratio in one-part geopolymer concrete and associated the high ratio with a balance between extrudability and buildability [18]. This finding supports the broader principle that aggregate loading can be deliberately increased when the particle size distribution and paste rheology are properly controlled. For the present 600 µm sand and BM-15 binder, the fixed 1.5 ratio is a defensible starting point, but further optimization would require direct comparisons at 1.25, 1.50, 1.75 and higher ratios under the same printing conditions.

4.14 Activator content: literature-based interpretation

The sodium metasilicate anhydrous activator content was fixed at 10% of binder. Activator dosage controls alkalinity, dissolution of aluminosilicate precursors and the rate of reaction-product formation. Too little activator may lead to incomplete activation and inadequate strength, while excessive activator can accelerate structural build-up, shorten open time and modify rheological behavior [8, 14-17].

Previous one-part geopolymer studies have used solid sodium silicate or related activators in the range relevant to the present 10% dosage and have shown that activator type and dosage can strongly influence printability [7, 8]. Muthukrishnan et al. reported 10% activator in a successful one-part printable formulation, while Bong et al. demonstrated that the grade of sodium silicate powder affects open time and hardened performance [7, 8]. The present 10% sodium metasilicate dosage is therefore consistent with established printable one-part geopolymer practice, but the optimum nature of the dosage should be understood as conditional on the chosen precursor chemistry and water content.

4.15 Comparison with recent literature

The present results align with several recent studies that emphasize the need to balance workability, setting and buildability. Tran et al. showed that slump and slump flow can be used as a simplified preliminary assessment of one-part geopolymer printability [12]. Their study demonstrates that a printable region is defined by a combination of flow-related measures rather than by one value. This supports the present selection procedure, where the post-drop flow and 10-min retention are considered together.

Bong et al. demonstrated the practical potential of just-add-water geopolymer concrete using solid sodium silicate powders and showed that open time, buildability and compressive strength can be simultaneously improved through material design [7]. Muthukrishnan et al. further established the importance of reaction kinetics, activator content and sucrose dosage in one-part geopolymer rheology [8]. These findings provide a direct scientific basis for the present choice of sodium metasilicate powder and sucrose.

More recent studies have moved beyond static mixture optimization toward process-integrated control. Chen et al. used sodium carbonate and nano-silica to extend printable time and improve large-scale printing potential [14]. Chen et al. also reported that nanocellulose and MgO can modify thixotropy, open time, shrinkage and strength [15]. Sheng et al. developed an extrusion device incorporating mixing and stirring to address the conflict between pumpability and buildability [16]. These developments suggest that BM-15 can serve as a material baseline for future printer-level optimization.

The newest literature also emphasizes systematic printable-window frameworks and lower-paste formulations [17, 18]. The emerging direction is therefore to integrate mixture chemistry, rheology, printing parameters and time into a single process window. The present work contributes to this direction by establishing a clearly defined candidate mix from a controlled 27-mixture screening program using accessible laboratory tests.

V. PROPOSED 3D-PRINTING PERFORMANCE FRAMEWORK FOR BM-15

4.1 Pumping stage

Before printing, BM-15 should be assessed under the actual pump and hose configuration. The target is continuous material transport without pressure spikes, segregation or blockage. The 600 µm maximum aggregate size provides a conservative particle-size condition for extrusion through a fine nozzle, while the intermediate w/b ratio should reduce pressure demand relative to the 0.30 mixtures. During pumping, the material should remain sufficiently mobile and should not be allowed to stand for excessive periods before reaching the nozzle.

4.2 Extrusion stage

At the nozzle, BM-15 should produce a continuous filament with a relatively uniform cross-section. The flow-table response indicates that the material is neither extremely stiff nor excessively fluid. Extrusion trials should quantify filament continuity, surface tearing, width variation and nozzle pressure. A successful filament should show minimal discontinuity and limited lateral spreading immediately after deposition.

4.3 Deposition and buildability

Immediately after extrusion, BM-15 must transition from a flowable state to a self-supporting state. The 50:50 FA:GGBS ratio is expected to assist this transition through the reactive slag fraction, while the 1.0% sucrose dosage prevents excessive acceleration of the early reaction. The 45-min setting-time window provides a useful material-level indication that structural development occurs over a practical period. The actual maximum layer count, however, must be experimentally measured because buildability also depends on nozzle size, layer height, print speed and interlayer time.

4.4 Shape retention

Shape retention should be quantified by measuring the width and height of each deposited layer. The key failure modes are lateral spreading, local bulging, layer waviness and cumulative dimensional drift. BM-15 is expected to show better shape retention than w/b = 0.40 mixtures because its initial flow is lower and its reaction rate is moderated. Conversely, it should be easier to extrude than w/b = 0.30 mixtures.

4.5 Open time

A practical printing trial should establish the time from mixing to the first observable loss of extrudability and the maximum interlayer interval before a cold joint becomes apparent. Although the setting-time results indicate a long material-level window, open time is not identical to setting time. Printing open time should be determined directly by repeated extrusion or time-dependent flow testing. This distinction is recognized in recent geopolymer printing literature [1, 4, 5, 14].

4.6 Recommended validation experiment

Conceptual relationship between fresh-state material requirements and the extrusion-based 3D-printing sequence is presented in Fig. 7. For final confirmation of BM-15, a cylindrical or wall-shaped object should be printed using a controlled nozzle diameter, constant layer height and fixed print speed. At least three deposition intervals should be examined. The printed specimen should be evaluated for layer width, total height, ovality or dimensional deviation, visible surface discontinuity, nozzle pressure, material continuity and maximum stable layer count. Mechanical specimens should be extracted or printed in multiple orientations to quantify anisotropy and interlayer strength. This would provide direct evidence connecting the laboratory screening results to actual 3D-printing performance.

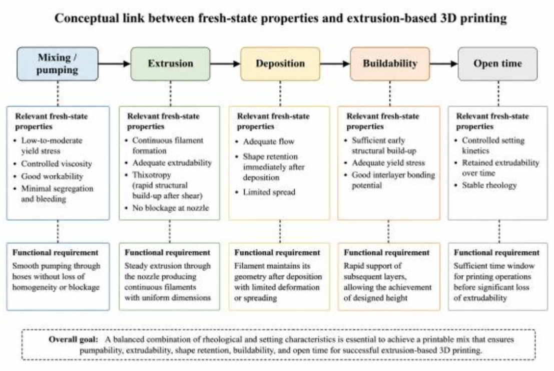

Figure 7. Conceptual relationship between fresh-state material requirements and the extrusion-based 3D-printing sequence.

VI. LIMITATIONS AND SCOPE OF INTERPRETATION

The principal limitation of the present study is that the results contain fresh-state screening, setting time, density and compressive strength of mold-cast specimens, but does not provide quantitative printer measurements such as extrusion pressure, rheometer-derived yield stress, plastic viscosity, thixotropic rebuilding rate, printed layer deformation, maximum layer count or interlayer bond strength. Consequently, the terms pumpability, extrudability and buildability are interpreted mechanistically from the measured properties and supported by the literature rather than claimed as directly measured values.

A second limitation is that aggregate-to-binder ratio and activator content were fixed. Future work should use BM-15 as the baseline and vary aggregate-to-binder ratio, activator dosage, nozzle geometry, print speed and interlayer time.

A third limitation is that no direct environmental assessment was provided. The use of fly ash and GGBS provides a pathway toward lower-clinker construction materials, but a rigorous carbon assessment would require source-specific data for precursor processing, activator manufacture, transportation, electricity and curing. Such analysis should be undertaken before making quantitative environmental claims.

VII. CONCLUSIONS

1. A one-part geopolymer concrete suitable for further extrusion-based 3D-printing development was formulated using fly ash, GGBS, sodium metasilicate anhydrous powder, fine sand and sucrose. Twenty-seven mixtures were evaluated by varying FA:GGBS ratio, water-to-binder ratio and sucrose dosage while keeping activator content at 10% and aggregate-to-binder ratio at 1.5.

2. Water-to-binder ratio was the dominant control on immediate flow. The w/b = 0.30 mixtures generally exhibited insufficient flow, whereas w/b = 0.40 mixtures produced high initial flow but comparatively poorer retention classifications. The intermediate w/b = 0.35 condition provided the most balanced workability.

3. Increasing the GGBS fraction generally reduced the initial flow but increased the potential for structural development and hardened strength. The 50:50 FA:GGBS ratio became particularly effective when combined with intermediate water and retarder contents.

4. Sucrose influenced both flow and setting behaviour. Increasing the retarder dosage generally delayed setting, but the highest dosage did not produce the best overall printability. The optimum occurred at 1.0% sucrose within the investigated matrix.

5. BM-15, consisting of 50:50 FA:GGBS, w/b = 0.35 and 1.0% sucrose, was identified as the optimum mixture. It exhibited 156 mm flow before drop, 141 mm after drop, 15 mm flow reduction after 10 min, 151 min initial setting, 196 min final setting, 2180 kg/m³ density, and 24.58 and 36.42 MPa compressive strengths at 7 and 28 days, respectively.

6. BM-15 provides the most balanced combination of flowability, retention, setting-time window and strength among the 27 mixtures. Its selection is therefore more defensible than selecting a mixture solely on maximum flow or maximum compressive strength.

7. The 1.5 aggregate-to-binder ratio and 10% activator dosage were not varied experimentally. Literature indicates that both parameters can strongly influence pumpability, extrusion pressure, structural build-up and open time; their optimization should be conducted in future work using BM-15 as the baseline.

The present results demonstrate material-level suitability for further 3D-printing validation but do not constitute direct measurements of pumpability, extrudability or buildability. Actual printing trials should quantify extrusion pressure, filament continuity, shape retention, maximum layer count, open time and interlayer bond strength. Overall, BM-15 is recommended as the optimum formulation within the investigated design space for subsequent extrusion-based concrete 3D-printing trials.

REFERENCES

[1] V. Sakhare, M. Najar, and S. Deshpande, "Printing performance of 3D-printed geopolymer through pumpability–extrudability–buildability properties–a review," *Architectural Science Review,* vol. 69, no. 1, pp. 88-112, 2026, doi: https://doi.org/10.1080/00038628.2024.2445050.

[2] P. Barve, A. Bahrami, and S. Shah, "Geopolymer 3D printing: a comprehensive review on rheological and structural performance assessment, printing process parameters, and microstructure," *Front.*

Mater., vol. 10, p. 1241869, 2023, doi: https://doi.org/10.3389/fmats.2023.1241869.

[3] S. Paritala, K. K. Singaram, I. Bathina, M. A. Khan, and S. K. R. Jyosyula, "Rheology and pumpability of mix suitable for extrusion-based concrete 3D printing–A review," *Constr. Build. Mater.,* vol. 402, p. 132962, 2023, doi: https://doi.org/10.1016/j.conbuildmat.2023.132962.

[4] A. Fasihi and N. A. Libre, "From pumping to deposition: A Comprehensive review of test methods for characterizing concrete printability," *Constr. Build. Mater.,* vol. 414, p. 134968, 2024, doi: https://doi.org/10.1016/j.conbuildmat.2024.134968.

[5] W. Si, M. Khan, and C. McNally, "A comprehensive review of rheological dynamics and process parameters in 3D concrete printing," *Journal of Composites Science,* vol. 9, no. 6, p. 299, 2025, doi: https://doi.org/10.3390/jcs9060299.

[6] P. Barve, A. Bahrami, and S. Shah, "A Comprehensive Review on Effects of Material Composition, Mix Design, and Mixing Regimes on Rheology of 3D-Printed Geopolymer Concrete," *Open Constr. Build. Tech. J.,* vol. 18, 2024, doi: 10.2174/0118748368292859240313061706.

[7] S. H. Bong, M. Xia, B. Nematollahi, and C. Shi, "Ambient temperature cured 'just-add-water'geopolymer for 3D concrete printing applications," *Cem. Concr. Compos.,* vol. 121, p. 104060, 2021, doi: https://doi.org/10.1016/j.cemconcomp.2021.104060.

[8] S. Muthukrishnan, S. Ramakrishnan, and J. Sanjayan, "Effect of alkali reactions on the rheology of one-part 3D printable geopolymer concrete," *Cem. Concr. Compos.,* vol. 116, p. 103899, 2021, doi: https://doi.org/10.1016/j.cemconcomp.2020.103899.

[9] H. Zhong and M. Zhang, "3D printing geopolymers: A review," *Cem. Concr. Compos.,* vol. 128, p. 104455, 2022, doi: https://doi.org/10.1016/j.cemconcomp.2022.104455.

[10] M. H. Raza, R. Y. Zhong, and M. Khan, "Recent advances and productivity analysis of 3D printed geopolymers," *Additive Manufacturing,* vol. 52, p. 102685, 2022, doi: https://doi.org/10.1016/j.addma.2022.102685.

[11] M. Nodehi, T. Ozbakkaloglu, and A. Gholampour, "Effect of supplementary cementitious materials on properties of 3D printed conventional and alkali-activated concrete: A review," *Autom. Constr.,* vol. 138, p. 104215, 2022, doi: https://doi.org/10.1016/j.autcon.2022.104215.

[12] M. V. Tran, T. H. Vu, and T. H. Y. Nguyen, "Simplified assessment for one-part 3D-printable geopolymer concrete based on slump and slump flow measurements," *Case Stud. Constr. Mater.,* vol. 18, p. e01889, 2023, doi: https://doi.org/10.1016/j.cscm.2023.e01889.

[13] M. B. Jaji, K. A. Ibrahim, G. P. A. G. van Zijl, and A. J. Babafemi, "Thixotropic characterisation of slag modified 3D printable metakaolin based geopolymer composite," *Mater. Today: Proc.,* 2023, doi: https://doi.org/10.1016/j.matpr.2023.03.530.

[14] Y. Chen, K. Xia, Z. Jia, Y. Gao, Z. Zhang, and Y. Zhang, "Extending applicability of 3D-printable geopolymer to large-scale printing scenario via combination of sodium carbonate and nano-silica," *Cem. Concr. Compos.,* vol. 145, p. 105322, 2024, doi: https://doi.org/10.1016/j.cemconcomp.2023.105322.

[15] Y. Chen *et al.*, "Rheology control and shrinkage mitigation of 3D printed geopolymer concrete using nanocellulose and magnesium oxide," *Constr. Build. Mater.,* vol. 429, p. 136421, 2024, doi: https://doi.org/10.1016/j.conbuildmat.2024.136421.

[16] Z. Sheng *et al.*, "Development of a novel extrusion device to improve the printability of 3D printable geopolymer concrete," *J. Build. Eng.,* vol. 88, p. 109079, 2024, doi: https://doi.org/10.1016/j.jobe.2024.109079.

[17] A. Afshin and A. Behnood, "3D Printing of Geopolymers and Alkali-Activated Materials: A Printable-Window Framework for Mix Design and Process Control," *J. Build. Eng.,* p. 116648, 2026, doi: https://doi.org/10.1016/j.jobe.2026.116648.

[18] B. L. Ajayi, G. P. van Zijl, and A. J. Babafemi, "High-strength low paste volume ternary-blended 3D printed one-part geopolymer concrete: rheology, hardened mechanics, and microstructure," *J. Sustainable Cem.-Based Mater.,* pp. 1-19, 2026, doi: https://doi.org/10.1080/21650373.2026.2674127.

[19] X. Zhu *et al.*, "Effect of microwave heating under varying exposure conditions on rheological properties, interlayer bond and buildability performance of 3D-printed geopolymer," *Constr. Build. Mater.,* vol. 486,

p. 141945, 2025, doi: https://doi.org/10.1016/j.conbuildmat.2025.141945.

[20] R. Liu *et al.*, "Industrial waste in 3D printed concrete: A mechanistic review on rheological control and printability," *J. Build. Eng.,* p. 114033, 2025, doi: https://doi.org/10.1016/j.jobe.2025.114033.

[21] S. Muthukrishnan, S. Ramakrishnan, and J. Sanjayan, "In-line activation of geopolymer slurry for concrete 3D printing," *Cem. Concr. Res.,* vol. 162, p. 107008, 2022, doi: https://doi.org/10.1016/j.cemconres.2022.107008.